

FIGO Staging System for Endometrial Cancer: Added Benefits of MR Imaging¹

Peter Beddy, FFRRCSI, FRCR • Ailbhe C. O'Neill, MB, BCh • Adam K. Yamamoto, MB, BS, MRCP • Helen C. Addley, MRCP, FRCR • Caroline Reinhold, MD, MSc • Evis Sala, MD, PhD, FRCR

ONLINE-ONLY CME

See www.rsna.org/education/lrg_cme.html

LEARNING OBJECTIVES

After completing this journal-based CME activity, participants will be able to:

- List the revisions included in the 2009 FIGO staging system for endometrial cancer.
- Describe the appearance of endometrial cancer at MR imaging.
- Discuss the use of diffusion-weighted and dynamic contrast-enhanced MR imaging for endometrial cancer staging.

TEACHING POINTS

See last page

Endometrial cancer is the most commonly diagnosed gynecologic malignancy in the United States. This pathologic condition is staged with the International Federation of Gynecology and Obstetrics (FIGO) system. The FIGO staging system recently underwent significant revision, which has important implications for radiologists. Key changes incorporated into the 2009 FIGO staging system include simplification of stage I disease and removal of cervical mucosal invasion as a distinct stage. Magnetic resonance (MR) imaging is essential for the preoperative staging of endometrial cancer because it can accurately depict the depth of myometrial invasion, which is the most important morphologic prognostic factor and correlates with tumor grade, presence of lymph node metastases, and overall patient survival. Diffusion-weighted MR imaging and dynamic contrast medium-enhanced MR imaging are useful adjuncts to standard morphologic imaging and may improve overall staging accuracy.

©RSNA, 2012 • radiographics.rsna.org

Abbreviations: ADC = apparent diffusion coefficient, FIGO = International Federation of Gynecology and Obstetrics

RadioGraphics 2012; 32:241–254 • Published online 10.1148/rg.321115045 • Content Codes: **GU** **MR** **OB** **OI**

¹From the Department of Clinical Radiology, University of Cambridge and Cambridge University Hospitals NHS Foundation Trust, Hills Road, Cambridge CB2 0QQ, England (P.B., A.K.Y., H.C.A., E.S.); Department of Radiology, St Vincent's University Hospital, Dublin, Ireland (A.C.O.); and Department of Radiology, McGill University Health Centre, Montreal, Quebec, Canada (C.R.). Presented as an education exhibit at the 2010 RSNA Annual Meeting. Received March 8, 2011; revision requested April 25 and received June 16; accepted June 30. For this journal-based CME activity, the author C.R. has disclosed a financial relationship (see p 253); all other authors, the editor, and reviewers have no relevant relationships to disclose. **Address correspondence to** P.B. (e-mail: pbeddy@eircom.net).

Introduction

Endometrial cancer is the fourth most common malignancy in females and the most common malignancy of the female reproductive tract (1). There were an estimated 43,470 new cases and approximately 7950 deaths from endometrial cancer in the United States in 2010 (2). The prevalence of endometrial cancer is increasing due to an aging population combined with rising levels of obesity (3). Approximately 75% of cases occur in postmenopausal women, with the median age at diagnosis being 70 years. Adenocarcinomas account for 90% of endometrial neoplasms, whereas uterine sarcomas are relatively rare and account for only 2%–6%; the remaining histologic types include adenocarcinoma with squamous cell differentiation and adenosquamous carcinoma (4,5). Endometrial cancer is staged with the International Federation of Gynecology and Obstetrics (FIGO) system, which recently underwent a major revision (6).

Prognosis depends on a number of factors, including stage, depth of myometrial invasion, lymphovascular invasion, histologic grade, and nodal status. **Depth of myometrial invasion is the most important morphologic prognostic factor**, correlating with tumor grade, presence of lymph node metastases, and overall patient survival. The prevalence of lymph node metastases increases from 3% with superficial myometrial invasion to 46% with deep myometrial invasion (7,8). Consequently, preoperative information about depth of myometrial invasion and histologic grade is essential in tailoring the surgical approach for these patients. Magnetic resonance (MR) imaging can accurately help assess the depth of myometrial invasion, whereas histologic grade can be determined with endometrial sampling. This information allows the selection of patients for pelvic or paraaortic lymph node sampling while obviating radical surgery in patients with a low risk of recurrent disease or significant comorbidities. Lymphadenectomy for early-stage (stage I) endometrial cancer remains controversial. Two large prospective multicenter studies investigated whether pelvic lymphadenectomy could improve the survival of women with early-stage endometrial cancer. Both studies reported no benefit in overall or recurrence-free survival in the patients randomized to lymphadenectomy (9,10). The recent SEPAL study (*survival effect of paraaortic lymphadenectomy in endometrial cancer*) showed

that pelvic and paraaortic lymphadenectomy improves outcome in patients with an intermediate or high risk of recurrent disease (11). The authors of this study acknowledged that MR imaging findings are an important predictor of lymph node metastases and, when combined with tumor grade and histologic findings, could be useful in selecting patients at low risk for recurrence (11). MR imaging can also allow accurate assessment of more advanced disease such as cervical stromal invasion or adnexal involvement. Additional information from an MR imaging staging examination (eg, uterine size, tumor volume, presence of ascites or adnexal disease) may help determine whether the surgical approach should be transabdominal, transvaginal, or laparoscopic.

Diffusion-weighted and dynamic multiphase contrast medium-enhanced MR imaging sequences have been shown to improve the accuracy of MR imaging in assessing the depth of myometrial invasion and can be used to assess tumor response to therapy and to differentiate tumor recurrence from posttreatment changes (12–14). In this article, we discuss the MR imaging assessment of endometrial cancer in terms of imaging protocol, recent modifications to the FIGO staging system, imaging appearances, and the complementary roles of diffusion-weighted and dynamic contrast-enhanced MR imaging.

MR Imaging Protocol

The patient should void approximately 1 hour before the examination to ensure that the bladder is only partially filled, since a full bladder may degrade T2-weighted MR images (5). An antiperistaltic agent such as hyoscine butyl bromide or glucagon is administered to reduce artifact from small bowel peristalsis. Alternatively, the patient can fast for 4–6 hours before the procedure, although in our experience, almost all patients require an antiperistaltic agent, even if they have been fasting (5). At our institution, the MR imaging studies are performed on a 1.5-T magnet (Signa Excite; GE Healthcare, Waukesha, Wis) with an eight-channel cardiac array coil. All imaging is performed with the patient supine. Axial, axial oblique, and sagittal fast recovery fast spin-echo T2-weighted images and axial T1-weighted images of the pelvis are obtained (Table 1). **All axial oblique images are obtained in a plane perpendicular to the endometrial cavity (5,12,14)**. Sagittal and axial oblique diffusion-weighted MR imaging of the pelvis is performed with *b* values of 0, 500 (sagittal), and 800 (axial oblique) sec/mm² (Table 1).

Teaching
Point

Teaching
Point

Table 1
MR Imaging Technique for Endometrial Cancer Staging

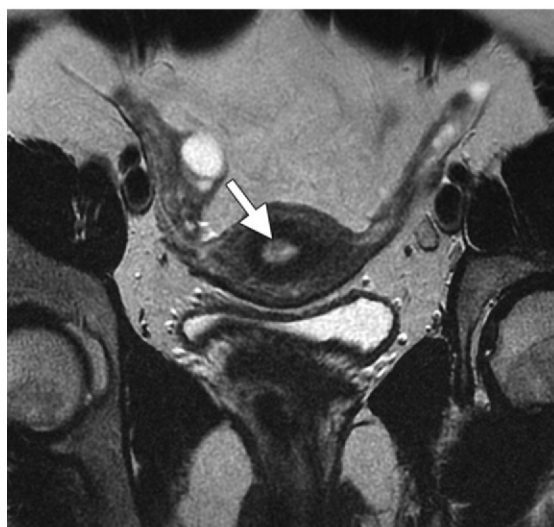
Parameter	Pulse Sequence															
	Axial T1W		Axial T2W		Sagittal T2W		Oblique T2W		Sagittal DW		Axial Oblique DW		Sagittal Multiphase DCE		Axial Oblique Multiphase DCE	
Sequence	FSE	FRFSE	EP	EP	EP	EP	GRE	GRE	GRE	GRE						
Repetition time (msec)	470	4500	4500	4500	4500	4500	4500	4500	5000	5000	5000	5000	6.4	6.4	6.4	6.4
Echo time (msec)	16	85	85	85	85	85	85	85	85	85	85	85	2.1	2.1	2.1	2.1
No. of signals acquired	2	3	4	4	4	4	4	4	6	6	6	6	1	1	1	1
No. of dimensions	2	2	2	2	2	2	2	2	2	2	2	2	3	3	3	3
Section thickness (mm)	5	5	5	5	5	5	5	5	4.5	4.5	4.5	4.5	4	4	4	4.2
Gap (mm)	2.5	2.5	2.5	2.5	2.5	2.5	0.5	0.5	0	0	0	0
Matrix size	448 × 288	384 × 256	384 × 256	384 × 256	384 × 256	384 × 256	384 × 256	128 × 128	128 × 128	128 × 128	128 × 128	128 × 128	288 × 192	288 × 192	288 × 192	288 × 192
Field of view (mm)	240	240	240	240	240	240	220	220	240	240	280	280	240	240	240	320
Bandwidth (kHz)	31.25	31.25	41.67	41.67	41.67	41.67	41.67	41.67	83.33	83.33	83.33	83.33
No. of sections	20	20	21	21	21	21	26	26	21	21	26	26	32 per volume slab	32 per volume slab	24 per volume slab	24 per volume slab
<i>b</i> Value (sec/mm ²)	500	500	800	800
Timing relative to contrast medium injection	Preinjection; 25 sec, 1 min, and 2 min after injection	Preinjection; 25 sec, 1 min, and 2 min after injection	Preinjection; 4 min after injection	Preinjection; 4 min after injection
Acquisition time*	4 min 50 sec	3 min 10 sec	3 min 10 sec	3 min 50 sec	4 min 30 sec	2 min 10 sec	2 min 10 sec	4 min 10 sec	4 min 10 sec	18 sec	18 sec	17 sec	17 sec			

Note.—DCE = dynamic contrast-enhanced, DW = diffusion-weighted, EP = echoplanar, FRFSE = fast recovery fast spin-echo, FSE = fast spin-echo, GRE = gradient-recalled echo, T1W = T1-weighted, T2W = T2-weighted.
*Varies depending on required coverage.

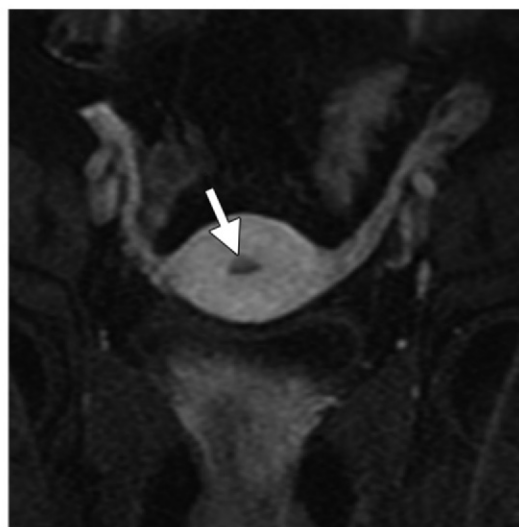
Figure 1. Stage IA endometrial cancer in a 35-year-old woman. **(a)** Sagittal T2-weighted MR image shows distention of the endometrial cavity by an intermediate-signal-intensity tumor (*). **(b)** Axial oblique T2-weighted MR image shows the intermediate-signal-intensity tumor (arrow) within the hyperintense endometrial cavity. The junctional zone is well delineated, with no evidence of invasion. **(c)** On an axial oblique dynamic contrast-enhanced MR image obtained 4 minutes after the intravenous injection of contrast medium, the tumor (arrow) is hypoenhancing relative to the hyperenhancing myometrium and appears to be confined to the endometrium.



a.



b.



c.

Dynamic contrast-enhanced MR images are obtained with a three-dimensional gradient-recalled echo T1-weighted LAVA (liver acquisition volume acceleration) sequence (GE Healthcare) after the administration of 0.1 mmol/kg of gadolinium at a rate of 2 mL/sec (5,12,14). Images are acquired prior to contrast medium injection and then during multiple phases of enhancement in both sagittal and axial oblique planes (sagittal: 25 sec, 1 min, and 2 min after

injection; axial oblique: 4 min after injection) (Table 1). Dynamic contrast-enhanced MR imaging is not performed in patients with renal impairment (estimated glomerular filtration rate <30). If advanced disease is suspected, axial imaging of the abdomen is also performed from the lung bases to the aortic bifurcation to assess for lymphadenopathy using a FIESTA (axial fast imaging employing steady-state acquisition [GE Medical Systems, Milwaukee, Wis]) or half-Fourier RARE (rapid acquisition with relaxation enhancement) sequence.

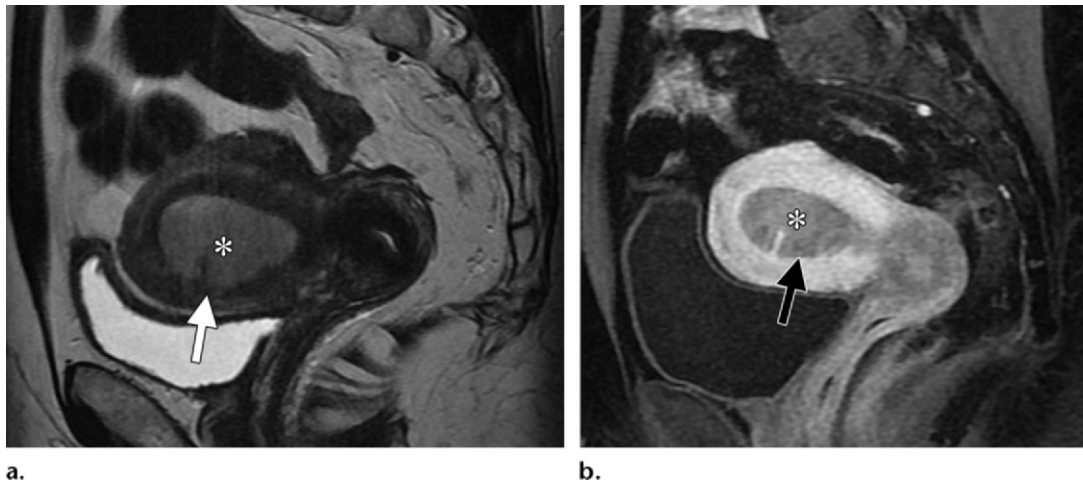


Figure 2. Stage IA endometrial cancer in a 61-year-old woman. **(a)** Sagittal T2-weighted MR image shows distention of the endometrial cavity by an intermediate-signal-intensity tumor (*). Poor tumor-to-myometrium contrast is seen inferiorly (arrow). **(b)** Sagittal dynamic contrast-enhanced MR image obtained 2 minutes after contrast medium injection demonstrates excellent contrast between the hyper-enhancing myometrium and the endometrial tumor (*), which appears to be confined to the endometrial cavity (arrow).

Table 2
2009 FIGO Staging System for Endometrial Cancer

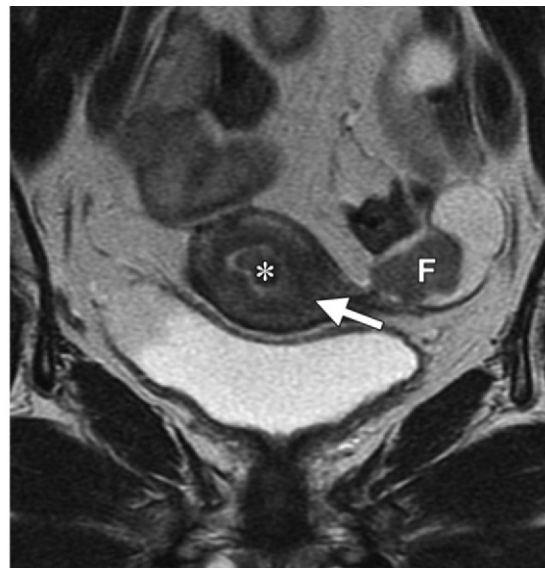
Stage	Description
IA	Tumor confined to uterus, <50% myometrial invasion
IB	Tumor confined to uterus, ≥50% myometrial invasion
II	Cervical stromal invasion
IIIA	Tumor invasion into serosa or adnexa
IIIB	Vaginal or parametrial involvement
IIIC1	Pelvic node involvement
IIIC2	Paraaortic node involvement
IVA	Tumor invasion into bladder or bowel mucosa
IVB	Distant metastases (including abdominal metastases) or inguinal lymph node involvement

FIGO Staging System

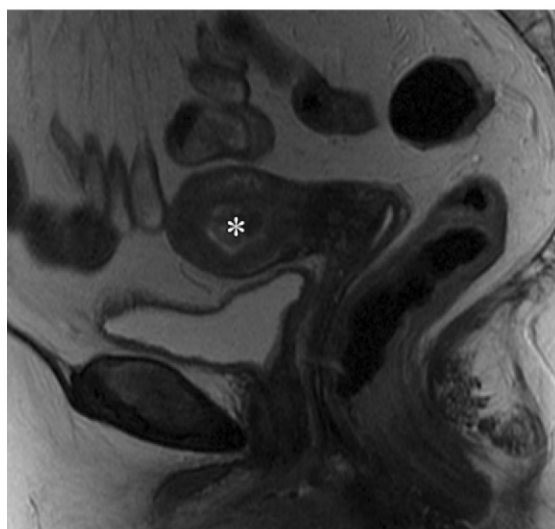
Surgical staging of endometrial cancer was first proposed in 1988, and the staging system was updated in 2009 (Table 2) (6). The previous iteration of the FIGO system subdivided stage I tumors into IA, IB, and IC tumors. Stage IA tumors were confined to the endometrial complex, stage IB tumors invaded only the inner half of the myometrium (<50% of the depth of

the myometrium), and stage IC tumors invaded the outer half of the myometrium (≥50% of the depth of the myometrium). In the 2009 revised FIGO staging system, tumors confined to the endometrium as well as those invading the inner half of the myometrium are designated as stage IA tumors (Figs 1–3) (6,15), and tumors

Figure 3. Stage IA endometrial cancer in a 72-year-old woman. **(a)** Axial oblique T2-weighted MR image demonstrates a hypointense tumor (*) that appears to be confined to the endometrium. The junctional zone is relatively poorly defined (arrow). A left ovarian fibroma (*F*) is incidentally noted. **(b)** Sagittal T2-weighted MR image shows the hypointense tumor (*) in the endometrial cavity. The junctional zone is poorly defined. **(c)** On an axial oblique dynamic contrast-enhanced MR image obtained 4 minutes after contrast medium injection, the endometrial tumor (*) is hypointense relative to the hyperintense enhancing myometrium, with invasion of the inner layer of the myometrium (arrows). Although the myometrial invasion is better depicted than on the T2-weighted images, this finding does not alter the stage in the new system. The left ovarian fibroma (*F*) has not enhanced.



a.



b.

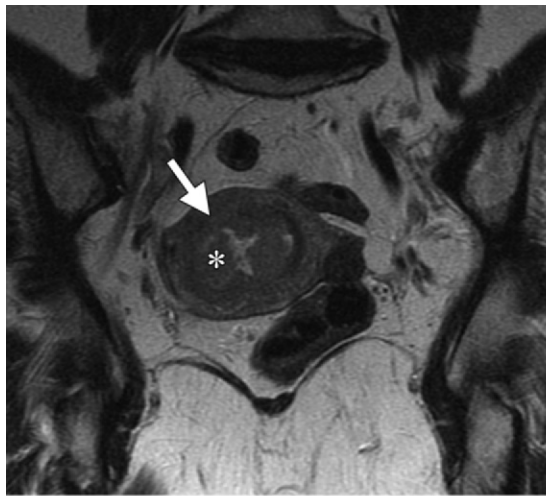


c.

invading the outer half of the myometrium are designated as stage IB tumors (Figs 4, 5). These changes may improve the diagnostic accuracy of MR imaging. With the old staging system, differentiating between stage IA and IB tumors could be challenging in patients with loss of junctional zone definition or in lesions with poor tumor-to-myometrium contrast, both of which are common pitfalls in endometrial cancer staging (Figs

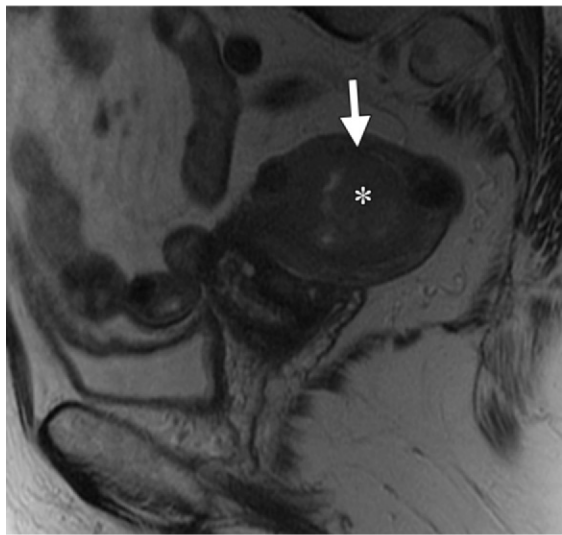
2, 3) (14,16,17). The amalgamation of stage IA and IB tumors into a new stage IA should alleviate this problem (Fig 3).

Stage II tumors were previously subdivided into stage IIA and IIB tumors, with IIA tumors characterized by endocervical glandular invasion and IIB tumors by cervical stromal invasion. The new system no longer has subsets IIA and IIB. Instead, tumors with endocervical glandular invasion are now considered stage I tumors, and tumors with cervical stromal invasion are defined as stage II tumors (Fig 6).



a.

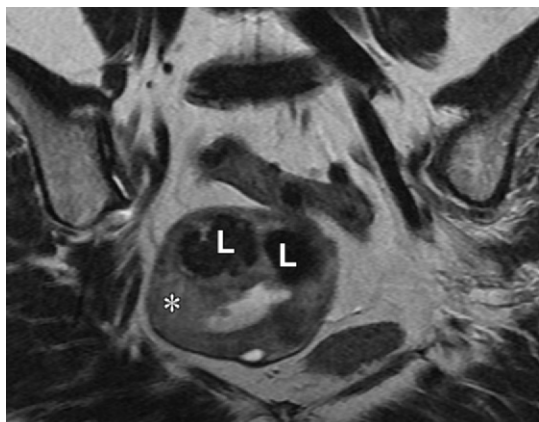
Figure 4. Stage IB endometrial cancer in a 53-year-old woman. **(a)** Axial oblique T2-weighted MR image demonstrates a tumor (*) with invasion of the myometrium. However, the depth of invasion is difficult to determine due to poor tumor-to-myometrium contrast (arrow). **(b)** Sagittal T2-weighted MR image shows a large iso- to hypointense endometrial tumor (*) with poor tumor-to-myometrium contrast (arrow). **(c)** Axial oblique dynamic contrast-enhanced MR image obtained 4 minutes after contrast medium injection shows tumor enhancement (*) with invasion of the outer half of the myometrium (arrow).



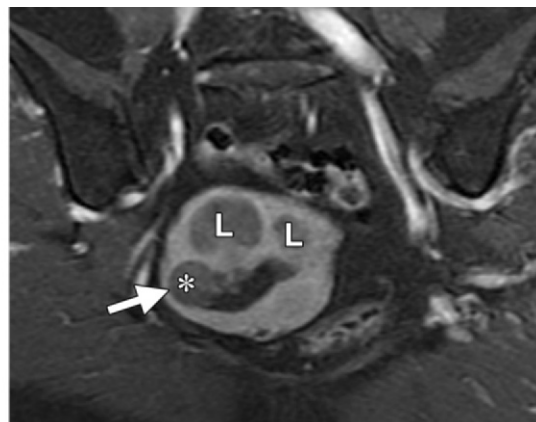
b.



c.



a.



b.

Figure 5. Stage IB endometrial cancer in a 71-year-old woman. **(a)** Axial oblique T2-weighted MR image demonstrates distention of the endometrial cavity by an ill-defined, isointense tumor (*) that extends into the myometrium. The depth of myometrial invasion is difficult to determine due to poor tumor-to-myometrium contrast. Two leiomyomas (*L*) are also present. **(b)** Axial oblique dynamic contrast-enhanced MR image obtained 4 minutes after contrast medium injection helps confirm deep myometrial invasion (arrow) by the tumor (*). The two leiomyomas (*L*) demonstrate enhancement.

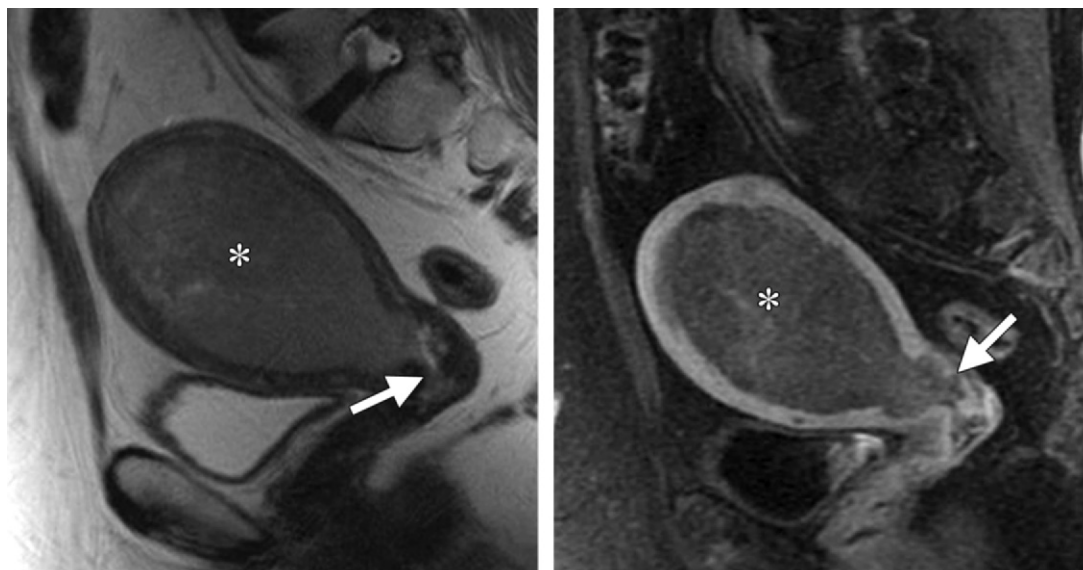
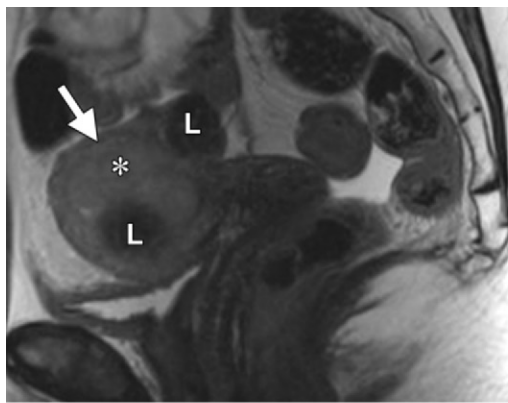


Figure 6. Stage II endometrial cancer in a 64-year-old woman. **(a)** Sagittal T2-weighted MR image shows distention of the endometrial cavity by a tumor (*) that extends into the cervix (arrow). **(b)** Sagittal dynamic contrast-enhanced MR image obtained 2 minutes after contrast medium injection shows extension of the endometrial tumor (*) into the cervix. Invasion of the cervical stroma is present posteriorly (arrow) and is better appreciated than on the T2-weighted image.

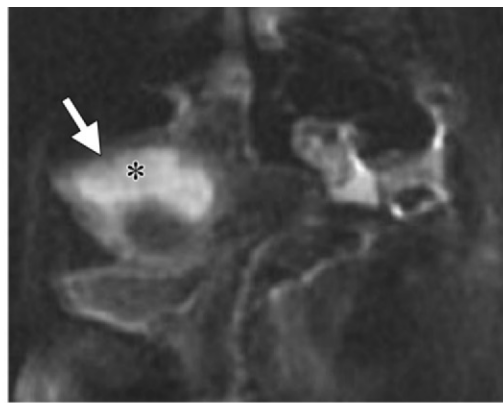
Stage III is still composed of three subdivisions: IIIA, IIIB, and IIIC. Stage IIIA tumors invade the serosa or adnexa (Fig 7), and stage IIIB tumors invade the vagina or parametrium (Fig 8). Previously, stage IIIC referred to any lymphadenopathy (pelvic or retroperitoneal); in the new FIGO system, however, stage IIIC is divided into stage IIIC1 (Fig 9), which is char-

acterized by pelvic lymph node involvement, and stage IIIC2 (Fig 10), which is characterized by paraaortic lymph node involvement. These changes reflect prognostic data that suggest a worse outcome in patients with involvement of paraaortic nodes than in those with involvement of pelvic nodes only (18). Stage IV remains unchanged: Stage IVA tumors (Fig 11) extend into adjacent bladder or bowel, and stage IVB tumors have distant metastases (eg, to the liver or lungs).

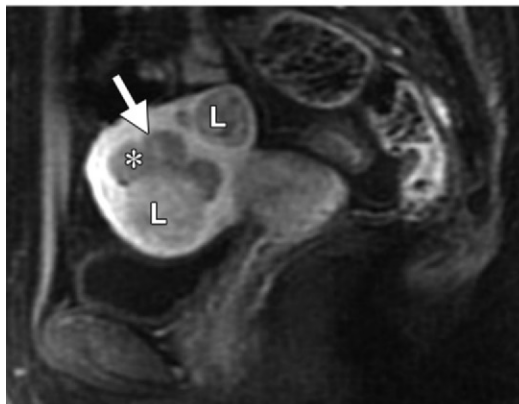
Figure 7. Stage IIIA endometrial cancer in a 65-year-old woman. **(a)** Sagittal T2-weighted MR image shows a large endometrial tumor (*). The depth of myometrial invasion is difficult to determine owing to poor tumor-to-myometrium contrast (arrow). In addition, the uterus is distorted by two leiomyomas (*L*), whose presence is a commonly reported pitfall in staging. **(b)** On a sagittal diffusion-weighted MR image ($b = 500 \text{ sec/mm}^2$), the tumor (*) has high signal intensity with deep myometrial invasion (arrow). **(c)** On a sagittal dynamic contrast-enhanced MR image obtained 2 minutes after contrast medium injection, the tumor (*) is hypointense relative to the hyperenhancing myometrium, with deep myometrial invasion (arrow). *L* = leiomyoma. **(d)** Axial oblique T2-weighted MR image shows extension of the endometrial tumor (*) into both fallopian tubes (arrows). The tumor is isointense relative to the adjacent myometrium. *L* = leiomyoma. **(e)** Axial oblique dynamic contrast-enhanced MR image obtained 4 minutes after contrast medium injection shows enhancement of the tumor extension into the fallopian tubes (arrows). The primary (endothelial) tumor (*) enhances less than the adjacent myometrium. **(f)** Axial oblique diffusion-weighted MR image ($b = 800 \text{ sec/mm}^2$) shows hyperintense tumor extension into the left fallopian tube and adnexa (arrowhead). The primary tumor (*) is bright relative to the adjacent myometrium. *O* = right ovary. **(g)** On an axial oblique apparent diffusion coefficient (ADC) map, the areas of high signal intensity seen at diffusion-weighted MR imaging demonstrate low signal intensity (*), a finding that is consistent with impeded diffusion. The tumor extension into the left fallopian tube (arrow) also exhibits impeded diffusion. The right ovary (*O*) remains bright (cf **f**), a finding that is consistent with T2 shine-through.



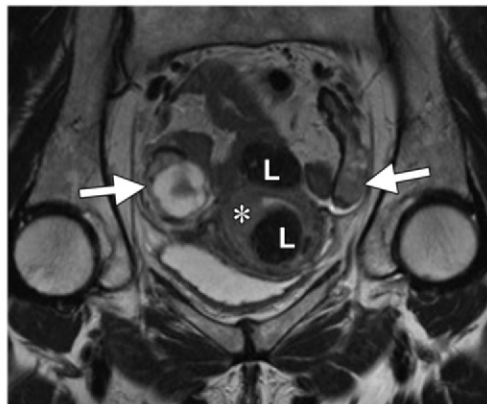
a.



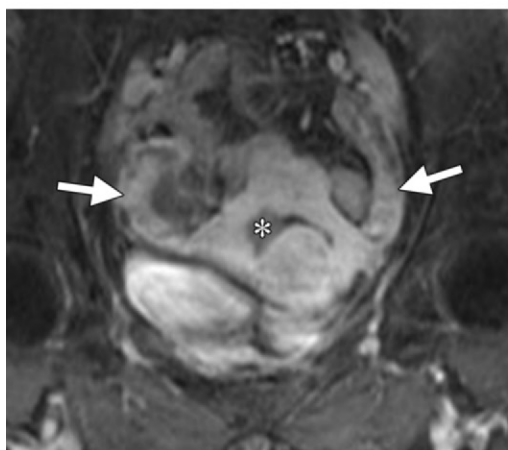
b.



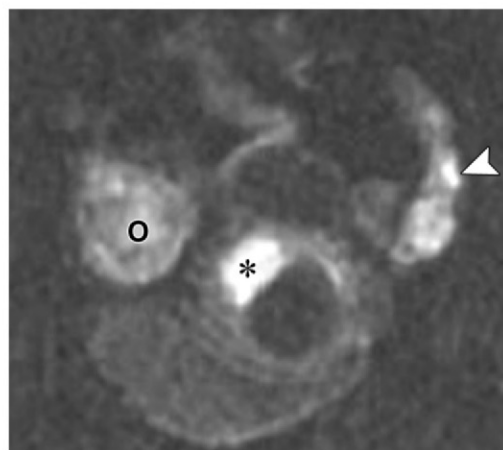
c.



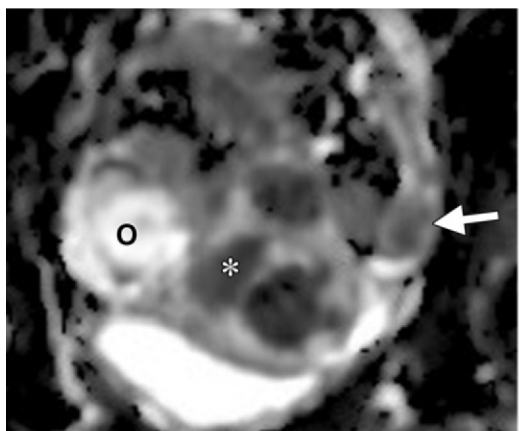
d.



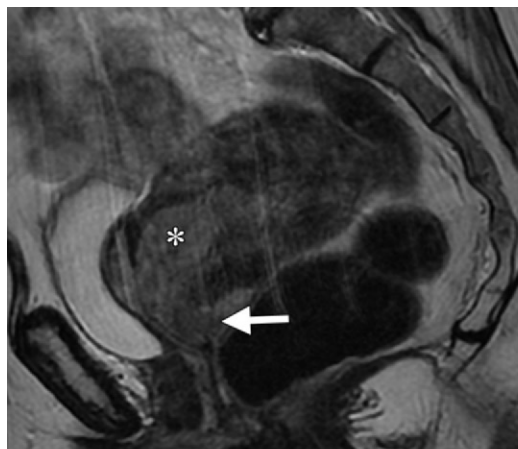
e.



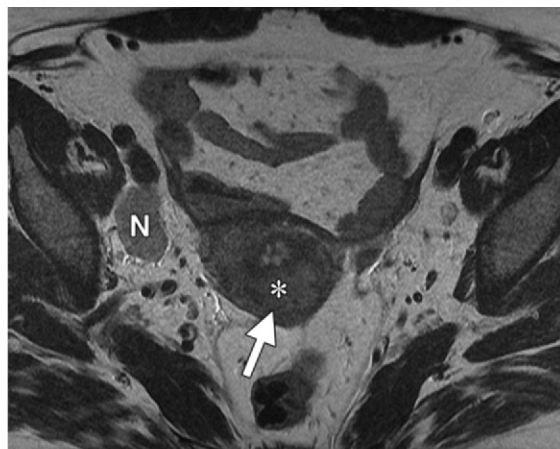
f.



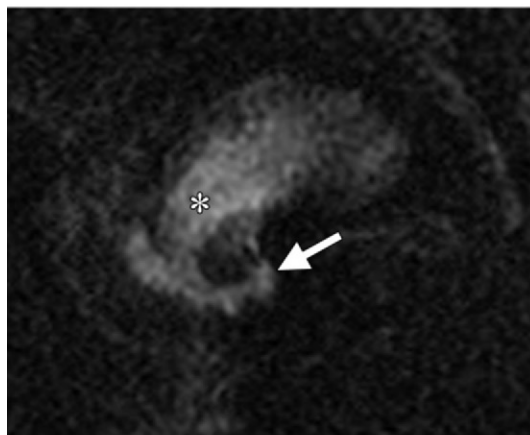
g.



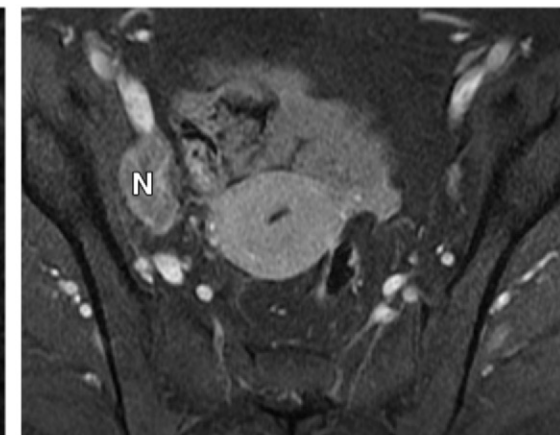
8a.



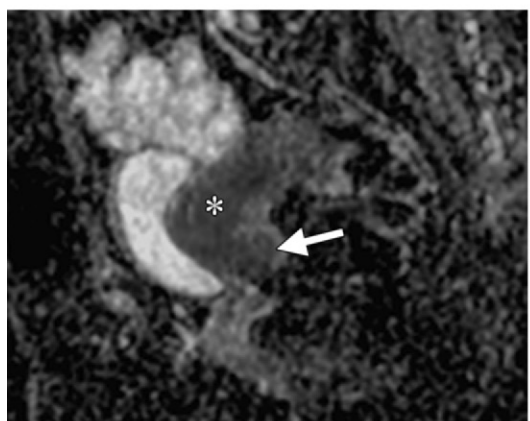
9a.



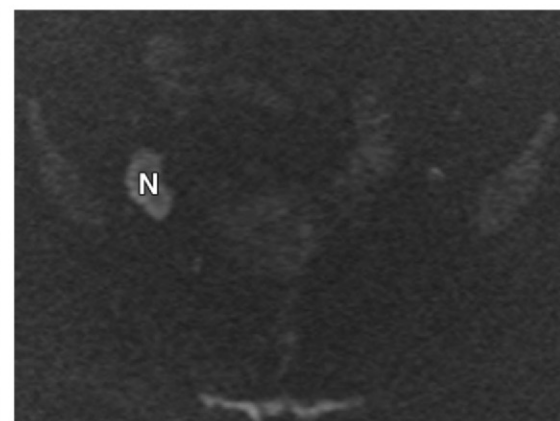
8b.



9b.



8c.



9c.

Figures 8, 9. (8) Stage IIIB endometrial cancer in an 80-year-old woman with chronic renal failure. (a) Sagittal T2-weighted MR image shows a large, isointense endometrial tumor (*) with extension into the upper aspect of the vagina (arrow). (b) On a sagittal diffusion-weighted MR image ($b = 500 \text{ sec/mm}^2$), the tumor (*) is hyperintense with invasion of the upper aspect of the vagina (arrow). (c) On a sagittal ADC map, the tumor (*) is hypointense due to impeded diffusion. Posterior vaginal invasion (arrow) is also noted. Although intravenous contrast medium was not administered in this case due to renal impairment, diffusion-weighted MR imaging was adequate for disease staging. (9) Stage IIIC1 endometrial cancer in a 66-year-old woman. (a) Axial T2-weighted MR image shows a bulky endometrial tumor (*) with poor tumor-to-myometrium contrast (arrow). An enlarged right external iliac lymph node (N) is also present. (b) On an axial dynamic contrast-enhanced MR image obtained 4 minutes after contrast medium injection, the node (N) demonstrates avid enhancement. (c) On an axial diffusion-weighted MR image ($b = 800 \text{ sec/mm}^2$), the node (N) demonstrates high signal intensity.

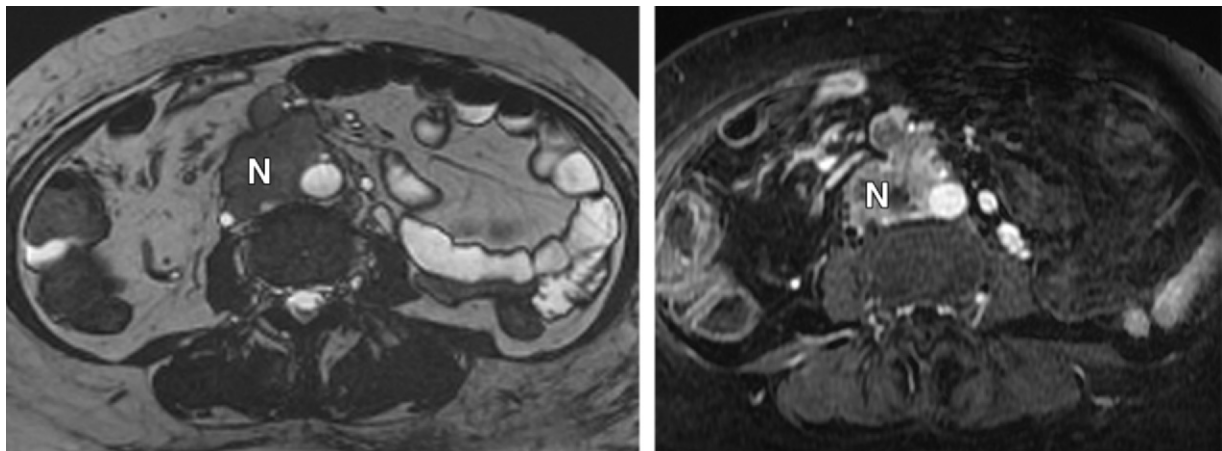


Figure 10. Stage IIIC2 endometrial cancer in a 74-year-old woman. **(a)** Axial FIESTA (axial fast imaging employing steady-state acquisition [GE Medical Systems]) image shows a large nodal mass (*N*) surrounding the inferior vena cava. **(b)** Axial dynamic contrast-enhanced MR image obtained 2 minutes after contrast medium injection demonstrates significant enhancement within the nodal mass (*N*).

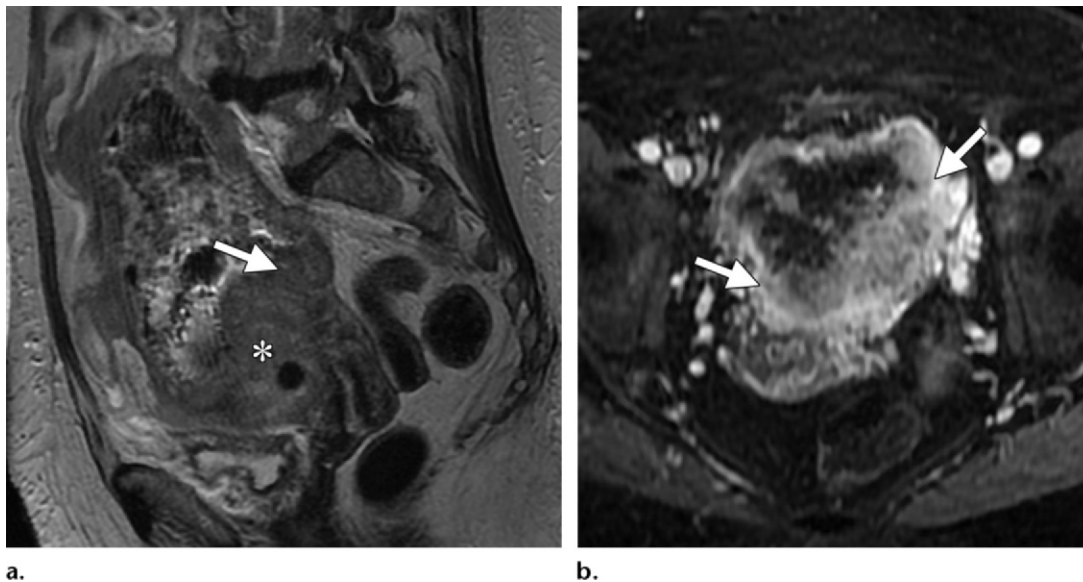


Figure 11. Stage IVA endometrial cancer in a 72-year-old woman. **(a)** Sagittal T2-weighted MR image shows a large endometrial tumor (*) with invasion of the sigmoid colon as evidenced by loss of the normal fat plane between the tumor and colon (arrow). **(b)** Axial dynamic contrast-enhanced MR image obtained 2 minutes after contrast medium injection shows invasion of the sigmoid colon (arrows) by the enhancing tumor, a finding that was confirmed at histopathologic analysis.

MR Imaging Appearances

Endometrial cancer is isointense relative to hypointense normal endometrium on unenhanced T1-weighted images and most commonly shows heterogeneous intermediate signal intensity relative to hyperintense normal endometrium on T2-weighted images (Figs 1–3) (5,19–21). Relative to normal myometrium, the tumor is mildly hyperintense on T2-weighted images. At conventional

MR imaging, the depth of myometrial invasion is optimally depicted with T2-weighted sequences. In the previous version of the FIGO staging system, breach or interruption of the junctional zone was important for differentiating between tumors confined to the endometrial complex and those invading the inner layer of the myometrium (Fig 3).

However, this finding may become less important now that confinement to the endometrial complex and inner myometrial invasion are both classified as stage IA (Fig 3). In postmenopausal women, there is thinning of the myometrium secondary to uterine involution, which can make accurate assessment of the depth of myometrial invasion challenging at conventional MR imaging (Fig 5) (22,23). Other commonly reported pitfalls in assessing the depth of myometrial invasion include tumor extension into the cornua, myometrial compression from a polypoid tumor, poor tumor-to-myometrium contrast (Fig 5), and the presence of leiomyomas (Fig 7) or adenomyosis (14,16,20,24). Morphologic imaging is of limited value in these cases, and the addition of diffusion-weighted and dynamic contrast-enhanced MR imaging sequences is extremely helpful in assessing the depth of myometrial invasion. The diagnostic accuracy of conventional MR imaging in this context ranges from 55% to 77% (17,22). Standard imaging is also significantly limited in its ability to help detect lymph node metastases. It relies on nodal size, shape, and internal architecture to help differentiate between benign and metastatic nodes, all of which features have been shown to be highly variable predictors of nodal involvement (25,26).

Added Value of Diffusion-weighted and Dynamic Contrast-enhanced MR Imaging

Dynamic contrast-enhanced MR imaging was first shown to improve the staging accuracy of MR imaging for endometrial cancer in the early 1990s (27). Differential enhancement within the endometrial cavity can allow tumor to be distinguished from blood products and debris (16,17,27,28). Endometrial tumors enhance earlier than does normal endometrium after the administration of intravenous contrast medium, which aids in the detection of small tumors confined to the endometrial complex. Normal myometrium enhances intensely compared with hypointense endometrial tumor (Figs 1–6). **Maximum contrast between hyperintense myometrium and hypointense endometrial tumor occurs 50–120 seconds after contrast medium administration**, and this is the most important phase for accurate assessment of the depth of myometrial invasion (Figs 2, 6) (17). Delayed-phase images obtained 3–4 minutes after contrast medium administration are useful in evaluating for cervical stromal invasion (FIGO stage II). The

presence of an intact enhancing cervical mucosa excludes stromal invasion.

The combination of dynamic contrast-enhanced and T2-weighted MR imaging offers a “one-stop” examination for endometrial cancer staging and is recommended by the European Society for Urological Research in its guidelines for endometrial cancer staging (22). Dynamic contrast-enhanced images, when read together with T2-weighted images, have a diagnostic accuracy of up to 98% for assessing myometrial invasion (12,14,16,17,22,29–33). However, there is some controversy in the literature regarding the added value of dynamic contrast-enhanced MR imaging for overall FIGO staging: Although the majority of published studies have shown an improvement in staging accuracy with dynamic contrast-enhanced MR imaging, some authors have found no benefit (14,16,17,22,29–31,34,35).

Diffusion-weighted MR imaging is a functional imaging technique that displays information about water mobility, tissue cellularity, and the integrity of the cell membranes (36–38). **Endometrial cancer exhibits impeded diffusion compared with surrounding tissue, manifesting with high signal intensity on diffusion-weighted MR images and low signal intensity on ADC maps, which provide a quantitative measure of water diffusion (Figs 7, 8) (38–41).** Diffusion-weighted MR images should always be reviewed with their corresponding ADC maps and other anatomic images to avoid pitfalls such as T2 shine-through (apparent high signal intensity of a lesion due to the long T2) (Fig 7). Impeded diffusion can also occur in areas of retained mucus such as an obstructed endometrial cavity, and cross-referencing with anatomic images can help differentiate this finding from tumor. In clinical practice, diffusion-weighted MR imaging should be performed with at least two b values: a low value of 0 or 50 sec/mm² and a high value of 500–1000 sec/mm² (13,40,42). The higher the b value, the less background signal and T2 shine-through will be present on the images. We have found a high b value of 800 sec/mm² to be optimal and use this b value for axial oblique diffusion-weighted MR imaging. We also use a third b value (500 sec/mm²) for sagittal imaging in the belief that it aids in assessing myometrial invasion and cervical stromal extension.

The added value of diffusion-weighted MR imaging for endometrial cancer staging is less well established than that of dynamic contrast-enhanced MR imaging; however, the diagnostic accuracy of diffusion-weighted MR imaging for assessing myo-

Teaching Point

Teaching Point

metrial invasion ranges from 62% to 90% (40,41). In a recent prospective study by Rechichi et al (13), the staging accuracy of diffusion-weighted MR imaging was superior to that of dynamic contrast-enhanced MR imaging and had a higher level of interobserver agreement. The authors suggested that diffusion-weighted MR imaging could replace dynamic contrast-enhanced MR imaging for endometrial cancer staging, offering the potential advantages of reduced scanning time and obviation of the intravenous administration of gadolinium-based contrast medium (Fig 8) (13). Diffusion-weighted imaging can also provide quantitative information in the form of ADC values. For calculation of ADC values, six or more b values should be used to ensure accurate quantification of impeded diffusion (42). Malignant tumors have significantly lower ADC values than benign lesions such as endometrial polyps and submucosal leiomyomas (39). Caution must be used because tumor necrosis in poorly differentiated lesions may also have high ADC values (38,41).

Impeded diffusion can occur in any normal anatomic structure with a high cellular density. Reactive lymph nodes may have high signal intensity at diffusion-weighted MR imaging due to their high cellular density, and impeded diffusion has been reported in both benign and metastatic lymph nodes (12,42). There are conflicting reports in the literature regarding the detection of lymph node metastases at diffusion-weighted MR imaging of gynecologic malignancies. Lin et al (43) demonstrated that 3.0-T MR imaging had a greater sensitivity in the detection of nodal metastases in patients with endometrial and cervical cancer. The authors reported that ADC values for malignant nodes were significantly lower than those for benign nodes, and that the use of nodal ADC values combined with lymph node size yielded a sensitivity of 83% for assessing the presence of nodal malignancy (43). In contrast, Nakai et al (44) used 1.5-T MR imaging to evaluate nodal ADC values in gynecologic malignancies and were unable to differentiate benign from malignant lymph nodes. However, they did find that diffusion-weighted MR imaging was useful in the detection of lymph nodes.

Conclusions

Significant changes have been made to the 2009 FIGO staging system for endometrial cancer, which has important implications for radiologists. Key changes include simplification of stage I disease and removal of cervical mucosal invasion as a distinct stage. Diffusion-weighted and dynamic

contrast-enhanced MR imaging are useful adjuncts to standard morphologic imaging and may improve overall staging accuracy.

Disclosures of Potential Conflicts of Interest.—C.R.:

Related financial activities: none. *Other financial activities:* consultant for Synarc.

References

1. National Cancer Institute. Cancer Stat Fact Sheets: corpus and uterus, NOS. Bethesda, Md: National Cancer Institute, 2010.
2. Jemal A, Siegel R, Xu J, Ward E. Cancer statistics, 2010. *CA Cancer J Clin* 2010;60(5):277–300.
3. Bray F, Dos Santos Silva I, Moller H, Weiderpass E. Endometrial cancer incidence trends in Europe: underlying determinants and prospects for prevention. *Cancer Epidemiol Biomarkers Prev* 2005;14(5):1132–1142.
4. Rha SE, Byun JY, Jung SE, et al. CT and MRI of uterine sarcomas and their mimickers. *AJR Am J Roentgenol* 2003;181(5):1369–1374.
5. Sala E, Wakely S, Senior E, Lomas D. MRI of malignant neoplasms of the uterine corpus and cervix. *AJR Am J Roentgenol* 2007;188(6):1577–1587.
6. Creasman W. Revised FIGO staging for carcinoma of the endometrium. *Int J Gynaecol Obstet* 2009;105(2):109.
7. Larson DM, Connor GP, Broste SK, Krawisz BR, Johnson KK. Prognostic significance of gross myometrial invasion with endometrial cancer. *Obstet Gynecol* 1996;88(3):394–398.
8. Berman ML, Ballon SC, Lagasse LD, Watring WG. Prognosis and treatment of endometrial cancer. *Am J Obstet Gynecol* 1980;136(5):679–688.
9. Benedetti Panici P, Basile S, Maneschi F, et al. Systematic pelvic lymphadenectomy vs. no lymphadenectomy in early-stage endometrial carcinoma: randomized clinical trial. *J Natl Cancer Inst* 2008;100(23):1707–1716.
10. Kitchener H, Swart AM, Qian Q, Amos C, Parmar MK. Efficacy of systematic pelvic lymphadenectomy in endometrial cancer (MRC ASTEC trial): a randomised study. *Lancet* 2009;373(9658):125–136.
11. Todo Y, Kato H, Kaneuchi M, Watari H, Takeda M, Sakuragi N. Survival effect of para-aortic lymphadenectomy in endometrial cancer (SEPAL study): a retrospective cohort analysis. *Lancet* 2010;375(9721):1165–1172.
12. Sala E, Rockall A, Rangarajan D, Kubik-Huch RA. The role of dynamic contrast-enhanced and diffusion weighted magnetic resonance imaging in the female pelvis. *Eur J Radiol* 2010;76(3):367–385.
13. Rechichi G, Galimberti S, Signorelli M, Perego P, Valsecchi MG, Sironi S. Myometrial invasion in endometrial cancer: diagnostic performance of diffusion-weighted MR imaging at 1.5-T. *Eur Radiol* 2010;20(3):754–762.

14. Sala E, Crawford R, Senior E, et al. Added value of dynamic contrast-enhanced magnetic resonance imaging in predicting advanced stage disease in patients with endometrial carcinoma. *Int J Gynecol Cancer* 2009;19(1):141–146.
15. Odicino F, Pecorelli S, Zigliani L, Creasman WT. History of the FIGO cancer staging system. *Int J Gynaecol Obstet* 2008;101(2):205–210.
16. Sironi S, Colombo E, Villa G, et al. Myometrial invasion by endometrial carcinoma: assessment with plain and gadolinium-enhanced MR imaging. *Radiology* 1992;185(1):207–212.
17. Yamashita Y, Harada M, Sawada T, Takahashi M, Miyazaki K, Okamura H. Normal uterus and FIGO stage I endometrial carcinoma: dynamic gadolinium-enhanced MR imaging. *Radiology* 1993;186(2):495–501.
18. Morrow CP, Bundy BN, Kurman RJ, et al. Relationship between surgical-pathological risk factors and outcome in clinical stage I and II carcinoma of the endometrium: a Gynecologic Oncology Group study. *Gynecol Oncol* 1991;40(1):55–65.
19. Chaudhry S, Reinhold C, Guermazi A, Khalili I, Maheshwari S. Benign and malignant diseases of the endometrium. *Top Magn Reson Imaging* 2003;14(4):339–357.
20. Hricak H, Rubinstein LV, Gherman GM, Karstaedt N. MR imaging evaluation of endometrial carcinoma: results of an NCI cooperative study. *Radiology* 1991;179(3):829–832.
21. Hricak H, Stern JL, Fisher MR, Shapeero LG, Winkler ML, Lacey CG. Endometrial carcinoma staging by MR imaging. *Radiology* 1987;162(2):297–305.
22. Manfredi R, Mirk P, Maresca G, et al. Local-regional staging of endometrial carcinoma: role of MR imaging in surgical planning. *Radiology* 2004;231(2):372–378.
23. Lee EJ, Byun JY, Kim BS, Koong SE, Shinn KS. Staging of early endometrial carcinoma: assessment with T2-weighted and gadolinium-enhanced T1-weighted MR imaging. *RadioGraphics* 1999;19(4):937–945; discussion 946–947.
24. Yamashita Y, Torashima M, Takahashi M, et al. Hyperintense uterine leiomyoma at T2-weighted MR imaging: differentiation with dynamic enhanced MR imaging and clinical implications. *Radiology* 1993;189(3):721–725.
25. McMahon CJ, Rofsky NM, Pedrosa I. Lymphatic metastases from pelvic tumors: anatomic classification, characterization, and staging. *Radiology* 2010;254(1):31–46.
26. Yang WT, Lam WW, Yu MY, Cheung TH, Metreweli C. Comparison of dynamic helical CT and dynamic MR imaging in the evaluation of pelvic lymph nodes in cervical carcinoma. *AJR Am J Roentgenol* 2000;175(3):759–766.
27. Hricak H, Hamm B, Semelka RC, et al. Carcinoma of the uterus: use of gadopentetate dimeglumine in MR imaging. *Radiology* 1991;181(1):95–106.
28. Ascher SM, Reinhold C. Imaging of cancer of the endometrium. *Radiol Clin North Am* 2002;40(3):563–576.
29. Ito K, Matsumoto T, Nakada T, Nakanishi T, Fujita N, Yamashita H. Assessing myometrial invasion by endometrial carcinoma with dynamic MRI. *J Comput Assist Tomogr* 1994;18(1):77–86.
30. Seki H, Kimura M, Sakai K. Myometrial invasion of endometrial carcinoma: assessment with dynamic MR and contrast-enhanced T1-weighted images. *Clin Radiol* 1997;52(1):18–23.
31. Nakao Y, Yokoyama M, Hara K, et al. MR imaging in endometrial carcinoma as a diagnostic tool for the absence of myometrial invasion. *Gynecol Oncol* 2006;102(2):343–347.
32. Kinkel K, Kaji Y, Yu KK, et al. Radiologic staging in patients with endometrial cancer: a meta-analysis. *Radiology* 1999;212(3):711–718.
33. Frei KA, Kinkel K, Bonél HM, Lu Y, Zaloudek C, Hricak H. Prediction of deep myometrial invasion in patients with endometrial cancer: clinical utility of contrast-enhanced MR imaging—a meta-analysis and Bayesian analysis. *Radiology* 2000;216(2):444–449.
34. Chung HH, Kang SB, Cho JY, et al. Accuracy of MR imaging for the prediction of myometrial invasion of endometrial carcinoma. *Gynecol Oncol* 2007;104(3):654–659.
35. Rockall AG, Meroni R, Sohaib SA, et al. Evaluation of endometrial carcinoma on magnetic resonance imaging. *Int J Gynecol Cancer* 2007;17(1):188–196.
36. Funt SA, Hricak H. Ovarian malignancies. *Top Magn Reson Imaging* 2003;14(4):329–337.
37. Koh DM, Collins DJ. Diffusion-weighted MRI in the body: applications and challenges in oncology. *AJR Am J Roentgenol* 2007;188(6):1622–1635.
38. Tamai K, Koyama T, Saga T, et al. Diffusion-weighted MR imaging of uterine endometrial cancer. *J Magn Reson Imaging* 2007;26(3):682–687.
39. Fujii S, Matsusue E, Kigawa J, et al. Diagnostic accuracy of the apparent diffusion coefficient in differentiating benign from malignant uterine endometrial cavity lesions: initial results. *Eur Radiol* 2008;18(2):384–389.
40. Lin G, Ng KK, Chang CJ, et al. Myometrial invasion in endometrial cancer: diagnostic accuracy of diffusion-weighted 3.0-T MR imaging—initial experience. *Radiology* 2009;250(3):784–792.
41. Shen SH, Chiou YY, Wang JH, et al. Diffusion-weighted single-shot echo-planar imaging with parallel technique in assessment of endometrial cancer. *AJR Am J Roentgenol* 2008;190(2):481–488.
42. Whittaker CS, Coady A, Culver L, Rustin G, Padwick M, Padhani AR. Diffusion-weighted MR imaging of female pelvic tumors: a pictorial review. *RadioGraphics* 2009;29(3):759–774; discussion 774–778.
43. Lin G, Ho KC, Wang JJ, et al. Detection of lymph node metastasis in cervical and uterine cancers by diffusion-weighted magnetic resonance imaging at 3T. *J Magn Reson Imaging* 2008;28(1):128–135.
44. Nakai G, Matsuki M, Inada Y, et al. Detection and evaluation of pelvic lymph nodes in patients with gynecologic malignancies using body diffusion-weighted magnetic resonance imaging. *J Comput Assist Tomogr* 2008;32(5):764–768.

FIGO Staging System for Endometrial Cancer: Added Benefits of MR Imaging

Peter Beddy, FFRRCSI, FRCR • Ailbhe C. O'Neill, MB, BCh • Adam K. Yamamoto, MB, BS, MRCP • Helen C. Addley, MRCP, FRCR • Caroline Reinhold, MD, MSc • Evis Sala, MD, PhD, FRCR

RadioGraphics 2012; 32:241–254 • Published online 10.1148/rg.321115045 • Content Codes: GU MR OB OI

Page 242

Depth of myometrial invasion is the most important morphologic prognostic factor.

Page 242

All axial oblique images are obtained in a plane perpendicular to the endometrial cavity (5,12,14).

Page 251 (Figure 1 on page 244. Figure 2 on page 245. Figure 3 on page 246.

Endometrial cancer is isointense relative to hypointense normal endometrium on unenhanced T1-weighted images and most commonly shows heterogeneous intermediate signal intensity relative to hyperintense normal endometrium on T2-weighted images (Figs 1–3) (5,19–21).

Page 252

Maximum contrast between hyperintense myometrium and hypointense endometrial tumor occurs 50–120 seconds after contrast medium administration.

Page 252 (Figure 7 on page 249. Figure 8 on page 250)

Endometrial cancer exhibits impeded diffusion compared with surrounding tissue, manifesting with high signal intensity on diffusion-weighted MR images and low signal intensity on ADC maps, which provide a quantitative measure of water diffusion (Figs 7, 8) (38–41).